Cell adhesion and migration

For adhesion assays, cells starved of cytokines for 24 h were washed and re-suspended in culture medium without cytokines. Cells were plated at 5×10^4 per well in a 50-μl volume in 96-well plates pre-coated overnight with 5 μg ml^{-1} human plasma fibronectin (Gibco). After 30 min of stimulation with or without SCF (in 100 μl final volume), non-adherent cells were removed by inverting plates for 15 min. The adherent cells were lysed using HTAB and β-hexosaminidase activity measured to assess the fraction of adherent cells. Adhesion is expressed as percentage of input. For migration assays, exponentially growing cells were washed and re-suspended in Tyrodes buffer. 10^5 cells were seeded in 100 μl in the upper chamber of 8-μm-pore-diameter transwells (BD Biosciences) with or without 100 ng ml^{-1} SCF in Tyrodes buffer in the lower chamber. After a 3–4-h incubation at 37 °C and 5% CO_2, the cells in the lower chamber were lysed using HTAB and β-hexosaminidase activity measured to assess the fraction of migrated cells.

Passive cutaneous anaphylaxis

The PCA protocols were adapted from refs 29, 30 (see Supplementary Information for detailed protocol).

Statistical analysis

All *in vitro* data shown are representative experiments (mean ± s.d.) from different BMMC cultures (established from at least 3–5 littermate mice each). Data for *in vitro* experiments were statistically analysed using a *t*-test and differences between wild-type and p110δ$^{D910A/D910A}$ BMMCs were statistically significant ($P < 0.05$) unless otherwise stated. Results from *in vivo* experiments (mean ± s.e.m.) were assessed using a Mann–Whitney *U*-test with results of analysis and animal numbers presented in the relevant figure legends. GraphPad Prism software was used for all statistical analyses.

Received 16 July; accepted 2 September 2004; doi:10.1038/nature02991.

1. Wedemeyer, J. & Galli, S. J. Mast cells and basophils in acquired immunity. *Br. Med. Bull.* **56,** 936–955 (2000).
2. Kinet, J. P. The high-affinity IgE receptor (FcεRI): from physiology to pathology. *Annu. Rev. Immunol.* **17,** 931–972 (1999).
3. Besmer, P. The kit ligand encoded at the murine Steel locus: a pleiotropic growth and differentiation factor. *Curr. Opin. Cell Biol.* **3,** 939–946 (1991).
4. Rivera, J. *et al.* Macromolecular protein signaling complexes and mast cell responses: a view of the organization of IgE-dependent mast cell signaling. *Mol. Immunol.* **38,** 1253–1258 (2002).
5. Serve, H. *et al.* Differential roles of PI3-kinase and Kit tyrosine 821 in Kit receptor-mediated proliferation, survival and cell adhesion in mast cells. *EMBO J.* **14,** 473–483 (1995).
6. Vanhaesebroeck, B. *et al.* Synthesis and function of 3-phosphorylated inositol lipids. *Annu. Rev. Biochem.* **70,** 535–602 (2001).
7. Lu-Kuo, J. M., Fruman, D. A., Joyal, D. M., Cantley, L. C. & Katz, H. R. Impaired kit- but not FcεRI-initiated mast cell activation in the absence of phosphoinositide 3-kinase p85α gene products. *J. Biol. Chem.* **275,** 6022–6029 (2000).
8. Vanhaesebroeck, B. *et al.* P110δ, a novel phosphoinositide 3-kinase in leukocytes. *Proc. Natl Acad. Sci. USA* **94,** 4330–4335 (1997).
9. Chantry, D. *et al.* p110δ, a novel phosphatidylinositol 3-kinase catalytic subunit that associates with p85 and is expressed predominantly in leukocytes. *J. Biol. Chem.* **272,** 19236–19241 (1997).
10. Okkenhaug, K. & Vanhaesebroeck, B. PI3K in lymphocyte development, differentiation and activation. *Nature Rev. Immunol.* **3,** 317–330 (2003).
11. Okkenhaug, K. *et al.* Impaired B and T cell antigen receptor signaling in p110δ PI 3-kinase mutant mice. *Science* **297,** 1031–1034 (2002).
12. Sadhu, C., Dick, K., Tino, W. T. & Staunton, D. E. Selective role of PI3K delta in neutrophil inflammatory responses. *Biochem. Biophys. Res. Commun.* **308,** 764–769 (2003).
13. Hinton, H. J. & Welham, M. J. Cytokine-induced protein kinase B activation and Bad phosphorylation do not correlate with cell survival of hemopoietic cells. *J. Immunol.* **162,** 7002–7009 (1999).
14. Tan, B. L. *et al.* Genetic evidence for convergence of c-Kit- and α4 integrin-mediated signals on class IA PI-3kinase and the Rac pathway in regulating integrin-directed migration in mast cells. *Blood* **101,** 4725–4732 (2003).
15. Tkaczyk, C., Beaven, M. A., Brachman, S. M., Metcalfe, D. D. & Gilfillan, A. M. The phospholipase Cγ1-dependent pathway of FcεRI-mediated mast cell activation is regulated independently of phosphatidylinositol 3-kinase. *J. Biol. Chem.* **278,** 48474–48484 (2003).
16. Fukao, T., Terauchi, Y., Kadowaki, T. & Koyasu, S. Role of phosphoinositide 3-kinase signaling in mast cells: new insights from knockout mouse studies. *J. Mol. Med.* **81,** 524–535 (2003).
17. Campbell, E., Hogaboam, C., Lincoln, P. & Lukacs, N. W. Stem cell factor-induced airway hyperreactivity in allergic and normal mice. *Am. J. Pathol.* **154,** 1259–1265 (1999).
18. Hundley, T. R. *et al.* Kit and FcεRI mediate unique and convergent signals for release of inflammatory mediators from human mast cells. *Blood* **104,** 2403–2417 (2004).
19. Strait, R. T., Morris, S. C., Yang, M., Qu, X. W. & Finkelman, F. D. Pathways of anaphylaxis in the mouse. *J. Allergy Clin. Immunol.* **109,** 658–668 (2002).
20. Fukao, T. *et al.* Selective loss of gastrointestinal mast cells and impaired immunity in PI3K-deficient mice. *Nature Immunol.* **3,** 295–304 (2002).
21. Chen, D. *et al.* p50α/p55α phosphoinositide 3-kinase knockout mice exhibit enhanced insulin sensitivity. *Mol. Cell. Biol.* **24,** 320–329 (2004).
22. Ueki, K. *et al.* Increased insulin sensitivity in mice lacking p85β subunit of phosphoinositide 3-kinase. *Proc. Natl Acad. Sci. USA* **99,** 419–424 (2002).
23. Terauchi, Y. *et al.* Increased insulin sensitivity and hypoglycaemia in mice lacking the p85α subunit of phosphoinositide 3-kinase. *Nature Genet.* **21,** 230–235 (1999).
24. Mauvais-Jarvis, F. *et al.* Reduced expression of the murine p85α subunit of phosphoinositide 3-kinase improves insulin signaling and ameliorates diabetes. *J. Clin. Invest.* **109,** 141–149 (2002).
25. Fruman, D. A. *et al.* Hypoglycaemia, liver necrosis and perinatal death in mice lacking all isoforms of phosphoinositide 3-kinase p85α. *Nature Genet.* **26,** 379–382 (2000).
26. Wymann, M. P., Zvelebil, M. & Laffargue, M. Phosphoinositide 3-kinase signalling–which way to target? *Trends Pharmacol. Sci.* **24,** 366–376 (2003).
27. Gray, A., Olsson, H., Batty, I. H., Priganica, L. & Peter Downes, C. Nonradioactive methods for the assay of phosphoinositide 3-kinases and phosphoinositide phosphatases and selective detection of signaling lipids in cell and tissue extracts. *Anal. Biochem.* **313,** 234–245 (2003).
28. Okayama, Y., Tkaczyk, C., Metcalfe, D. D. & Gilfillan, A. M. Comparison of FcεRI- and FcγRI-mediated degranulation and TNF-α synthesis in human mast cells: selective utilization of phosphatidylinositol-3-kinase for FcγRI-induced degranulation. *Eur. J. Immunol.* **33,** 1450–1459 (2003).
29. Tilley, S. L., Wagoner, V. A., Salvatore, C. A., Jacobson, M. A. & Koller, B. H. Adenosine and inosine increase cutaneous vasopermeability by activating A(3) receptors on mast cells. *J. Clin. Invest.* **105,** 361–367 (2000).
30. Laffargue, M. *et al.* Phosphoinositide 3-kinase gamma is an essential amplifier of mast cell function. *Immunity* **16,** 441–451 (2002).

Supplementary Information accompanies the paper on **www.nature.com/nature**.

Acknowledgements We thank R. Profit and G. Willams for bioanalytical support. K.A. and A.B. were supported in part by an MRC-CASE and Fondazione Italiana per la Ricerca sul Cancro fellowship, respectively. Research in the laboratory of B.V. is funded by the Ludwig Institute for Cancer Research, the Biotechnology and Biological Science Research Council and European Union FP5 and FP6 Programmes.

Competing interests statement The authors declare that they have no competing financial interests.

Correspondence and requests for materials should be addressed to B.V. (bartvanh@ludwig.ucl.ac.uk).

DNA end resection, homologous recombination and DNA damage checkpoint activation require CDK1

Grzegorz Ira[1]*, Achille Pellicioli[2]*, Alitukiriza Balijja[2], Xuan Wang[1]†, Simona Fiorani[2], Walter Carotenuto[2], Giordano Liberi[2], Debra Bressan[1], Lihong Wan[3], Nancy M. Hollingsworth[3], James E. Haber[1] & Marco Foiani[2]

[1]*Rosenstiel Center and Department of Biology, Brandeis University, Waltham, Massachusetts 02454-9110, USA*
[2]*F.I.R.C. Institute of Molecular Oncology Foundation, Via Adamello 16, 20139, Milano, Italy, and Dipartimento di Scienze Biomolecolari e Biotecnologie, Universitá degli Studi di Milano, Italy*
[3]*Department of Biochemistry and Cell Biology, SUNY Stony Brook, Stony Brook, New York 11794-5215, USA*

* These authors contributed equally to this work
† Present address: Rockefeller University, 1230 York Avenue, New York, New York 10021-6399, USA

A single double-strand break (DSB) induced by HO endonuclease triggers both repair by homologous recombination and activation of the Mec1-dependent DNA damage checkpoint in budding yeast[1–6]. Here we report that DNA damage checkpoint activation by a DSB requires the cyclin-dependent kinase CDK1 (Cdc28) in budding yeast. CDK1 is also required for DSB-induced homologous recombination at any cell cycle stage. Inhibition of homologous recombination by using an analogue-sensitive CDK1 protein[7,8] results in a compensatory increase in non-homologous end joining. CDK1 is required for efficient 5′ to 3′ resection of DSB ends and for the recruitment of both the single-stranded DNA-binding complex, RPA, and the Rad51 recombination protein. In contrast, Mre11 protein, part of the MRX complex, accumulates at unresected DSB ends. CDK1 is not required when the DNA damage checkpoint is initiated by lesions that are processed by nucleotide excision repair. Maintenance of the DSB-induced checkpoint requires continuing CDK1 activity that ensures continuing end resection. CDK1 is also important for a later step in homologous recombination, after strand invasion and before the initiation of new DNA synthesis.

In budding yeast, a chromosomal DSB created by HO endonuclease has been used both to study the kinetics and efficiency of DSB

repair and to analyse the induction of the DNA damage checkpoint dependent on Mec1 (an ATR homologue). In cells carrying *HML* or *HMR* mating-type switching donor sequences, a DSB at the *MAT* locus is efficiently repaired by gene conversion. In strains lacking donor sequences, induction of an unrepairable DSB causes arrest of cell cycle progression before anaphase[1,2]. In both instances, a key step is the 5′ to 3′ resection of DSB ends to produce single-stranded DNA (ssDNA), which is bound by the RPA complex. RPA binding is essential both for association of Mec1 checkpoint kinase[9] and for loading of Rad51 recombination protein[6].

Activation of the Mec1-dependent DNA damage checkpoint after a DSB is regulated by the cell cycle[3], with no activation in G1-arrested cells. A DSB induced in cells that have been arrested in G1, and then released into S phase, results in hyperphosphorylation of the Mec1 target Rad53 after the completion of S phase, in G2 (Supplementary Fig. S1a). To test whether the checkpoint depends on the activity of cyclin-dependent kinases, we inactivated CDK1 in nocodazole-blocked G2 cells. We overexpressed the CDK1/Clb inhibitor, Sic1 (ref. 10), in G2 cells at the same time that an unrepairable DSB was induced at *MAT*. CDK1 inactivation is measured by the progressive dephosphorylation of the B subunit of DNA polymerase-α, a marker for Cdc28/Clb activity[11] (Fig. 1). *SIC1* overexpression prevents the accumulation of phosphorylated Rad53 and Chk1 (Fig. 1) and impairs hyperphosphorylation of the upstream checkpoint factors Ddc2 and Rad9 as well as Mre11 (Fig. 1). Because the phosphorylation of Ddc2 and Rad9 is directly mediated by Mec1 kinase, we conclude that CDK1 inactivation affects Mec1.

To determine whether G1-arrested cells are able to perform homologous recombination (HR), we arrested *MAT***a** cells with α-factor and then induced a DSB with HO. Recombination between *HML*α and *MAT***a**, monitored by Southern blots, was nearly absent in comparison with that in cells growing exponentially or in cells arrested in G2 with nocodazole, where replacement of *MAT***a** by *MAT*α was efficient (Fig. 2a).

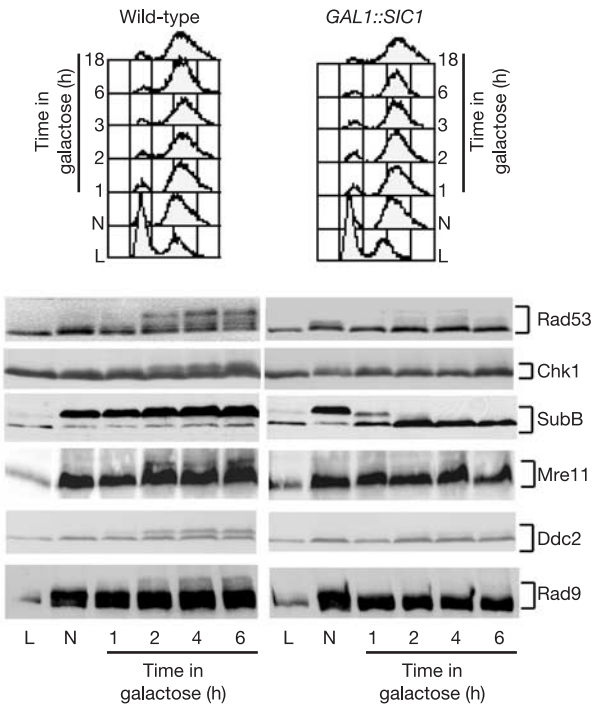

Figure 1 CDK1 activity is required for DSB-induced phosphorylation of checkpoint proteins in G2 cells. The phosphorylation of checkpoint proteins in the presence of an HO-induced unrepaired DSB in G2/M cells arrested with nocodazole (N) is shown, comparing cells with active CDK1 or *GAL::SIC1*-inactivated CDK1.

Inhibition of HR in G1-arrested cells was also seen in a diploid where a DSB at *MAT* could be repaired only by allelic recombination with an uncleavable *MAT***a**-inc locus on a homologous chromosome (Fig. 2e). We obtained similar inhibition of HO-induced recombination in G1 haploid cells when an HO-induced DSB was repaired by ectopic recombination between chromosomes III and V (ref. 5; data not shown).

To establish that the failure of HO-induced recombination in G1-arrested cells was attributable to a lack of Cdc28 activity, we examined recombination in cells expressing Cdc28-as1, a mutant sensitive to the ATP analogue inhibitor 1-NMPP1 (ref. 7). Galactose-induced HO cleavage was efficient, but cell-cycle-arrested cells failed almost completely to repair the DSB (Fig. 2b). 1-NMPP1 did not affect repair in wild-type cells (Fig. 2c).

CDK1 is also required for HR in the G2/M stage of cell cycle. We arrested *cdc28-as1* cells in G2 with nocodazole and then induced the expression of HO. Whereas recombination was normal in G2-arrested cells, *MAT* switching was nearly abolished in Cdc28-inhibited cells (Fig. 2b).

Failure of both checkpoint activation and HR in G1-arrested cells and in both Sic1-inhibited and Cdc28-as1-inhibited G2 cells correlates with an absence of 5′ to 3′ resection of DSB ends. The effect of overexpressing *GAL1::SIC1* in nocodazole-arrested G2 cells was shown by examining the rate of loss of the HO-cut *MAT***a** *Eco*RI restriction fragment in strains lacking *HML* or *HMR*, where the DSB is not repaired (Fig. 3a). Inhibiting CDK1 counteracted degradation of the HO-cut fragment as well as additional fragments a greater distance from the DSB. Resection was not significantly affected in G2-arrested cells deleted for Rad9, Rad17 or Mec1 checkpoint proteins[12] (data not shown).

Similar defects in resection were seen in α-factor-arrested G1 cells and in all stages of the cell cycle when Cdc28-as1 was inhibited (Fig. 3a). Without resection, HO-cleaved *MAT* sequences fail to bind either RPA or Rad51 (Fig. 3b and Supplementary Fig. S1) as determined by chromatin immunoprecipitation (ChIP). A similar failure of RPA loading was seen when CDK1 was inhibited by Sic1 overexpression (Fig. 3b). In contrast, both resection and RPA and Rad51 binding are seen in nocodazole-arrested G2 cells, in which CDK1 is active (Fig. 3b). Without RPA and Rad51 binding, HR should not occur. The absence of RPA recruitment to DSB ends in CDK1-inhibited cells also accounts for the failure to activate the Mec1-dependent DNA damage checkpoint, because Mec1-Ddc2 recruitment depends on prior binding of RPA[9].

The 5′ to 3′ resection of HO-induced DSB ends is reduced, but not eliminated, in cells deleted for *MRE11*, *RAD50* or *XRS2* (ref. 1). However, there are cell cycle differences in the control of resection. In G2-arrested cells, 5′ to 3′ resection depends almost completely on the MRX complex[13], but in G1-arrested cells there is still residual resection when *RAD50* is deleted (Fig. 3a). When Cdc28-as1 kinase was inhibited in wild-type G2-arrested cells, resection was as defective as in *rad50Δ* G2-arrested cells (Fig. 3a). We conclude that Cdc28 controls resection activity associated with the MRX complex. We note that Cdc2 in *Schizosaccharomyces pombe* has been suggested to control the resection of DSBs, but independently of Rad50 (ref. 14). Without resection, *mre11Δ* G2-arrested cells also fail to activate the DNA damage checkpoint[15] (Fig. 3c).

Because Mre11 is required for DSB resection and checkpoint activation[1,15,16], we asked whether defective resection caused by CDK1 inactivation reflects the inability to load Mre11 on broken chromosomes. We found Mre11 at DSBs in G2 cells (Fig. 3b and Supplementary Fig. S1), even when CDK1 is inactive. However, whereas in wild-type cells the amount of Mre11 crosslinked near the DSB declines by 2 h, in Sic1-overexpressing cells Mre11 remains associated with unresected ends. Transient association of Mre11 with DSB ends in wild-type cells might suggest that MRX proteins

migrate down DNA as resection proceeds; however, we could not detect significant association of Mre11 with DNA 5 kilobases (kb) from the HO cut even after several hours (when resection has reached and passed this region[6]) (data not shown). However, it is possible that Mre11 becomes spread out and undetectable. CDK1 inactivation therefore does not prevent Mre11 loading onto DSBs.

Although G1-arrested cells fail to perform efficient DSB-induced HR, they exhibit an increased efficiency of non-homologous end joining (NHEJ). In strains lacking *HML* or *HMR*, repair of the DSB occurs only by Ku- and DNA ligase 4-dependent rejoining of the 4-base-pair (bp) 3′-overhanging complementary HO-cleaved ends[17]. When 1-NMPP1 was added 30 min before 1 h of HO induction in growing cells, NHEJ increased fivefold, from 12% to 65% (Fig. 2f). The same increase in NHEJ was observed when CDK1 inhibitor was added to nocodazole-arrested G2 cells (Fig. 2f). These results support and extend previous suggestions[18,19] that the higher stability of DSB ends in G1-arrested cells stimulates NHEJ, which we propose might result from a lack of resection of these ends. In

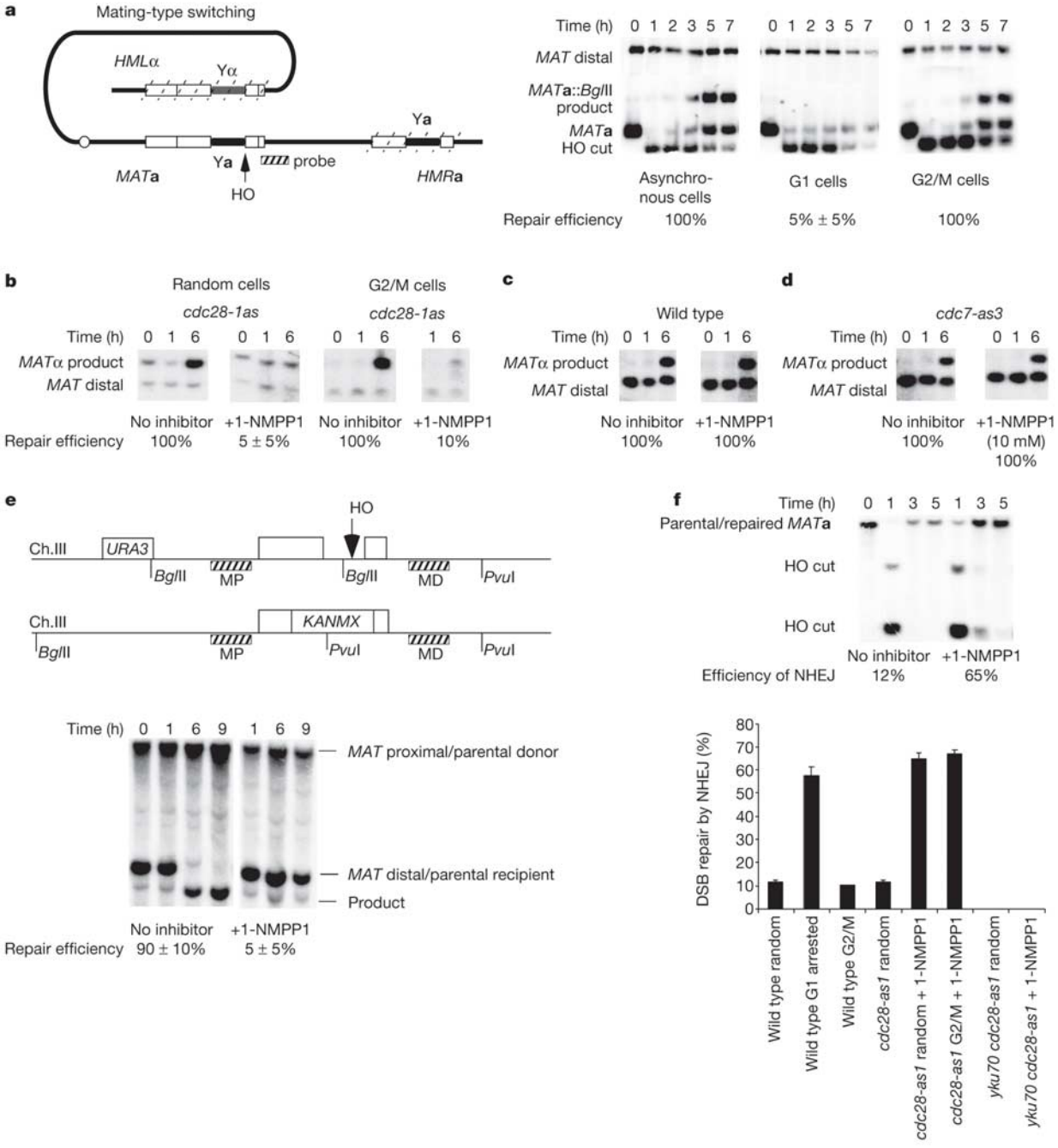

Figure 2 *CDK1* is required for homologous recombination. **a**, *MAT* switching is initiated by creating an HO-induced DSB at the *MAT* locus that is repaired by gene conversion from *HML* or *HMR*. *MAT* switching is shown in asynchronous cells or cells arrested in G1 (α-factor arrest) or G2/M (nocodazole arrest). **b**–**d**, *MAT* switching in *cdc28-as1* (**b**), wild-type (**c**) and *cdc7-as3* (**d**) strains with and without 1-NMPP1 inhibitor. **e**, Allelic recombination in a *cdc28-as1* homozygous diploid strain. The position of two DNA probes is shown: *MAT*-distal (MD, verifies DSB induction) and *MAT*-proximal (MP, detects product). **f**, Efficiency of NHEJ in *cdc28-as1* cells with either active or inactive *CDK1* at different stages of the cell cycle. Error bars indicate s.d.

addition, NHEJ is probably aided by the retention of the end-joining protein Mre11 at DSB ends (Fig. 3b).

Lack of checkpoint activation in CDK1-inhibited cells proves to be specific for DSB damage and not for other conditions that induce Mec1-dependent checkpoint activation. For example, G1 cells exposed to the ultraviolet-mimetic agent 4-nitroquinoline 1-oxide (4NQO) exhibit Rad53 phosphorylation[11] (Fig. 4a). CDK1 activity is therefore not required when the checkpoint is activated by presumably ssDNA intermediates of nucleotide excision repair. Furthermore, CDK1 inhibition does not affect checkpoint activation in response to S-phase arrest caused by hydroxyurea[20], during which ssDNA intermediates arise at stalled replication forks[21]. We conclude that CDK1 influences Mec1-dependent checkpoint activation only when the DNA damage involves DSBs that must be resected to generate ssDNA.

We tested whether CDK1 activity was required for the maintenance of the active checkpoint state and continuing DSB resection. DSB formation was induced in wild-type and *cdc28*-as1 G2 cells. Both strains promote robust checkpoint activation, but when Cdc28-as1 was inactivated by adding 1-NMPP1, both the checkpoint and DSB resection were turned off (Fig. 4b, c). When inhibitor is added, a region 20 kb from the DSB fails to be degraded (Fig. 4c). Hence, CDK1 is required for ongoing resection and for maintaining the checkpoint. Indeed we believe that the signal for checkpoint maintenance is not simply the presence of ssDNA but rather some event that is linked to the continuing resection process.

Beyond affecting the formation of ssDNA, CDK1 seems to have a second function during HR. First, although in G2-arrested cells both the *rad50Δ* mutation and inhibition of Cdc28-as1 have the same effect on resection (Fig. 3a), recombination still occurs at about 20% of wild type in *rad50Δ* cells but is completely abolished when Cdc28-as1 is blocked (data not shown). This suggests that Cdc28 must affect other steps in DSB repair. To examine CDK1's role more directly, we added inhibitor to *cdc28-as1* cells at intervals

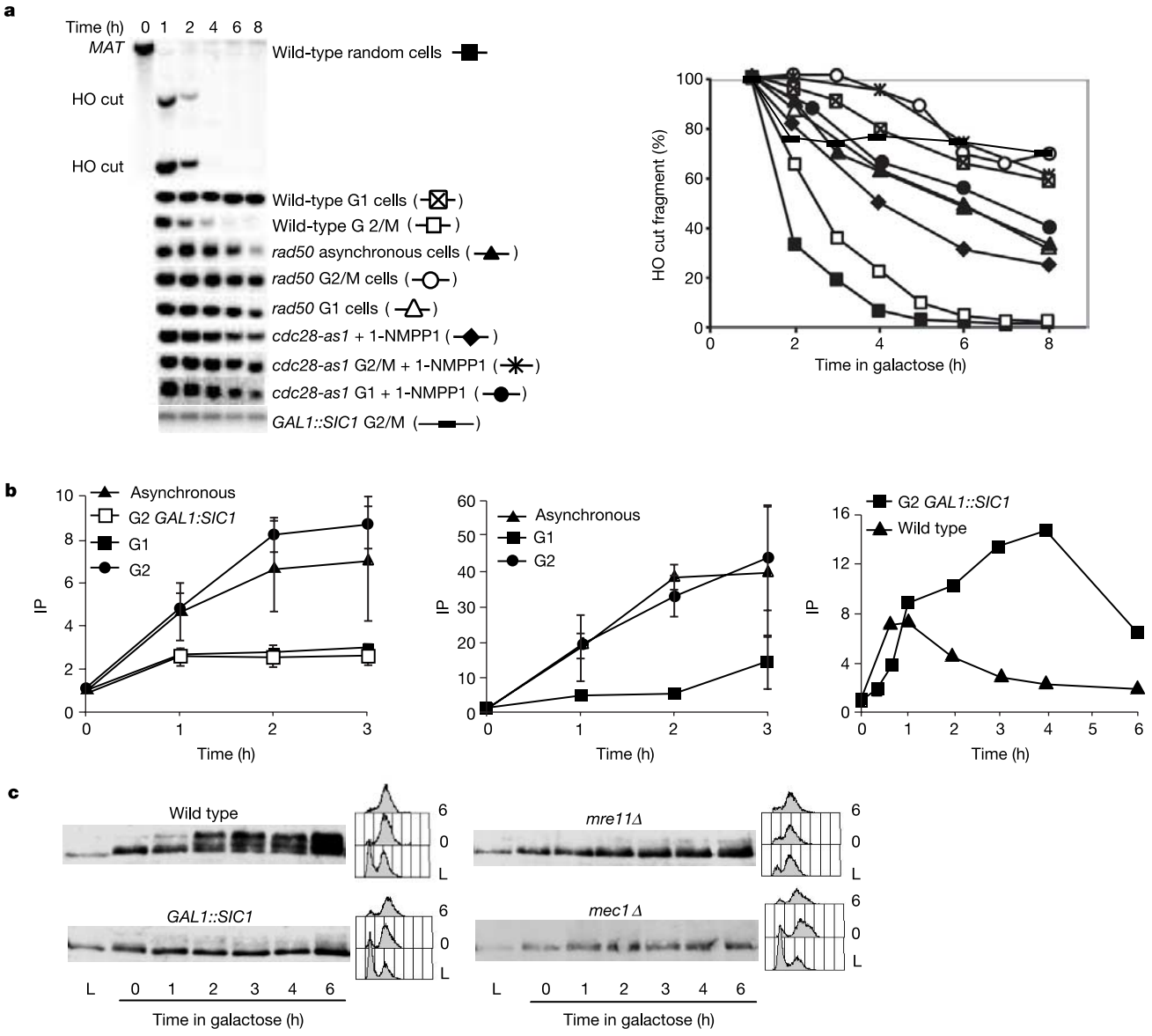

Figure 3 CDK1 is needed for DSB resection. **a**, The 5′ to 3′ resection of DSB ends was analysed in the indicated mutants and at different points in the cell cycle by loss of the HO-cut *Eco*RI restriction fragment in a strain lacking *HML* or *HMR*. **b**, ChIP analysis of binding of RPA (left), Rad51 (centre) and Mre11 (right) to DSB ends in a donorless strain[4,6], in asynchronous or G1 cells and in G2/M-arrested cells with or without Sic1 inhibition of CDK1. Where error bars are shown, results are means ± s.d. **c**, Lack of Rad53 phosphorylation in *mre11Δ* G2/M-arrested cells, compared with other conditions.

after initiation of HO cleavage. When inhibitor was added 4–6 h after break induction, the extent of repair was unaffected, but at earlier times the addition of inhibitor reduced the completion of DSB repair (Fig. 5a). The most striking results were found when inhibitor was added 2 h after DSB induction. By this time, most DSB ends have been resected sufficiently to bind both Rad51 and RPA[4,6]. This is evident from ChIP analyses showing that, by 90 min, RPA and Rad51 had bound near the HO cut as efficiently as in wild-type cells. Moreover, Rad51-ssDNA filaments succeeded in strand invasion and synapsis with the donor, so that the *HML* locus (200 kb from *MAT*) could be immunoprecipitated by anti-Rad51 antibody[4]. As shown in Fig. 5b and Supplementary Fig. S1, Rad51-mediated synapsis between *MAT* and *HML* was comparable to that seen without inhibitor at each time up to 4 h, when *MAT* switching is complete without inhibitor. However, the next step in repair, the initiation of new DNA synthesis (primer extension) from the 3′ end of the invading strand, was severely impaired in cells to which inhibitor was added (Fig. 5c and Supplementary Fig. S1). We conclude that CDK1 is required after synapsis and before the initiation of new DNA synthesis, a process that requires the loading of the proliferating cell nuclear antigen (PCNA) clamp and the recruitment of DNA polymerase.

The Cdc7 protein kinase is activated by CDK1 and is required for the initiation of DNA replication[22]. Using an analogue-sensitive allele of *CDC7*, *cdc7-as3*, we showed that HO-induced recombination is efficient in Cdc7-as3-inhibited cells (Fig. 2d). Thus, cells arrested in late G1, before the initiation of S phase but beyond the START point where CDK1 is activated, are capable of resecting DSB ends and completing HR.

Results presented here reveal a central role for budding yeast's CDK1, Cdc28, in the regulation of DSB repair. First, when CDK1 is inactive, in G1 cells before passing START, HR is markedly reduced, as it is in G1-stage mammalian cells. This observation is supported by the finding that G1-arrested yeast cells fail to form DNA-damage-induced foci of Rad52 protein[23]. Moreover, the DNA damage checkpoint, which requires extensive resection of DSB ends, is not activated in G1-arrested cells[3]. We note that HR is not completely abolished in G1-arrested or Cdc28-inhibited cells; there is still residual 5′ to 3′ resection of DSB ends (apparently by a Cdc28-independent exonuclease) and about 5–10% of product is still formed. The CDK1-dependent regulation of HR and NHEJ might also help to explain the cell-cycle specificity of DSB repair in mammalian cells. Mammalian G1 cells predominantly repair ionizing radiation damage by NHEJ[24]. Similarly, V(D)J recombination by NHEJ during lymphoid development is restricted to G0/G1 phases of the cell cycle by the tight regulation of *RAG2* gene expression and protein degradation. When *RAG2* is expressed throughout the cell cycle it causes aberrant recombination products involving HR[25]. Once cells have passed START, HR is activated, allowing DSBs arising during replication to be repaired efficiently by HR.

We show that CDK1 is required for the establishment and maintenance of the Mec1/Rad53-mediated checkpoint response after DSB formation and for initiating and sustaining Mre11-dependent DSB resection. CDK1-mediated DSB resection influences checkpoint activation by allowing the formation of RPA-ssDNA filaments. Mre11 loading at DSB ends is not in itself sufficient to promote checkpoint activation, suggesting that Mec1-dependent checkpoint activation is instead influenced by the Mre11-mediated formation of RPA filaments. A tantalizing possibility is that in G2 CDK1 regulates the phosphorylation state of the MRX complex and/or other as yet unidentified factors implicated in DSB processing. Indeed several proteins implicated in DNA recombination are targeted by CDKs, including Xrs2, RPA and Srs2 (refs 8, 20). However, we note that neither *mre11*-T294V/S379A/S413A/T529V/S560A/T677V nor *xrs2*-T108V/S542A (in which the putative Cdc28-dependent phosphorylation sites have been mutagenized) exhibit hypersensitivity to DNA-damaging agents or appreciable defects in checkpoint activation after a DSB in G2 (data not shown). CDKs have been also implicated in the phosphorylation of checkpoint proteins (namely Rad9, Drc1/Sld2, Ddc1, Dun1 and Ptc3)[8,26,27]; however, it is not known whether these phosphorylation events have any role in checkpoint activation or rather in recovery from damage.

A hypothesis suggested by our data is that CDK1 has a key function in regulating alternative DSB repair pathways (NHEJ or HR) in G1 and G2. Hence, CDK1 inactivation in G2 seems to

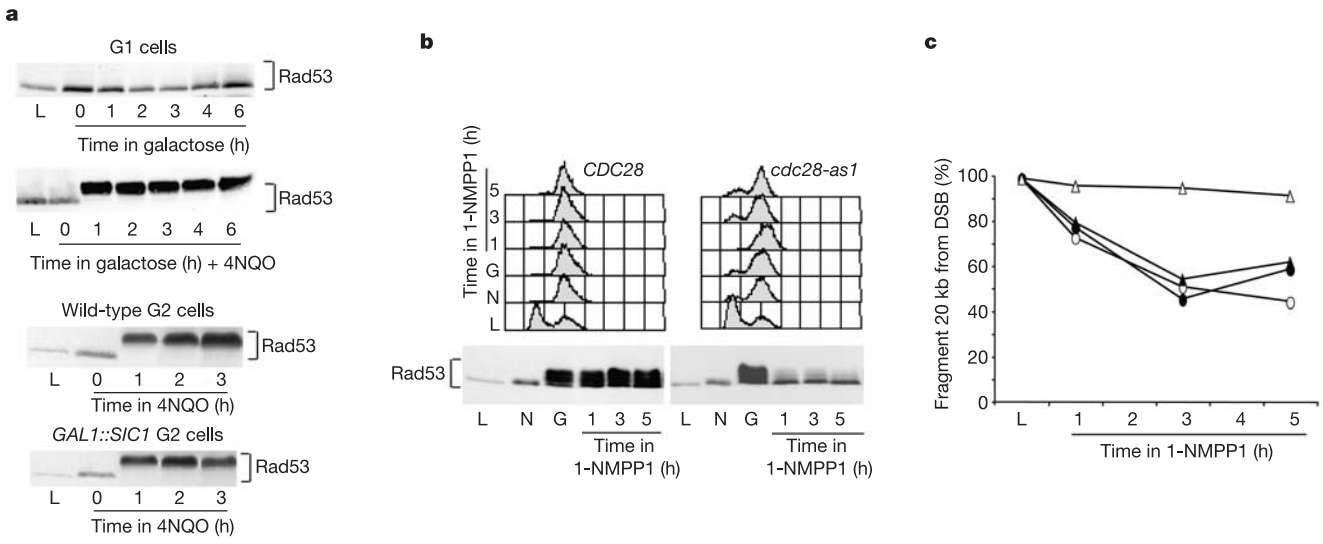

Figure 4 CDK1 is required to maintain Rad53 activation in response to a DSB but not after damage by 4NQO. **a**, In G1-arrested cells, Rad53 is not phosphorylated when an HO-mediated DSB is induced by galactose, but is triggered when 4NQO provokes nucleotide excision repair. In nocodazole-arrested G2/M cells, treatment with 4NQO causes Rad53 phosphorylation even when CDK1 is inhibited by Sic1. **b**, At 6 h after DSB induction, when the checkpoint is established and Rad53 is phosphorylated, 1-NMPP1 was added to either *CDC28* or *cdc28-as1* strains. **c**, Rad53 phosphorylation is lost when CDK1 is inactivated, and resection of a *Sty*I fragment, 20 kb from the DSB, is inhibited. Open triangles, *cdc28-as1* G2 + 1-NMPP1, filled triangles, *cdc28-as1* G2, open circles, wild type G2 + 1-NMPP1.

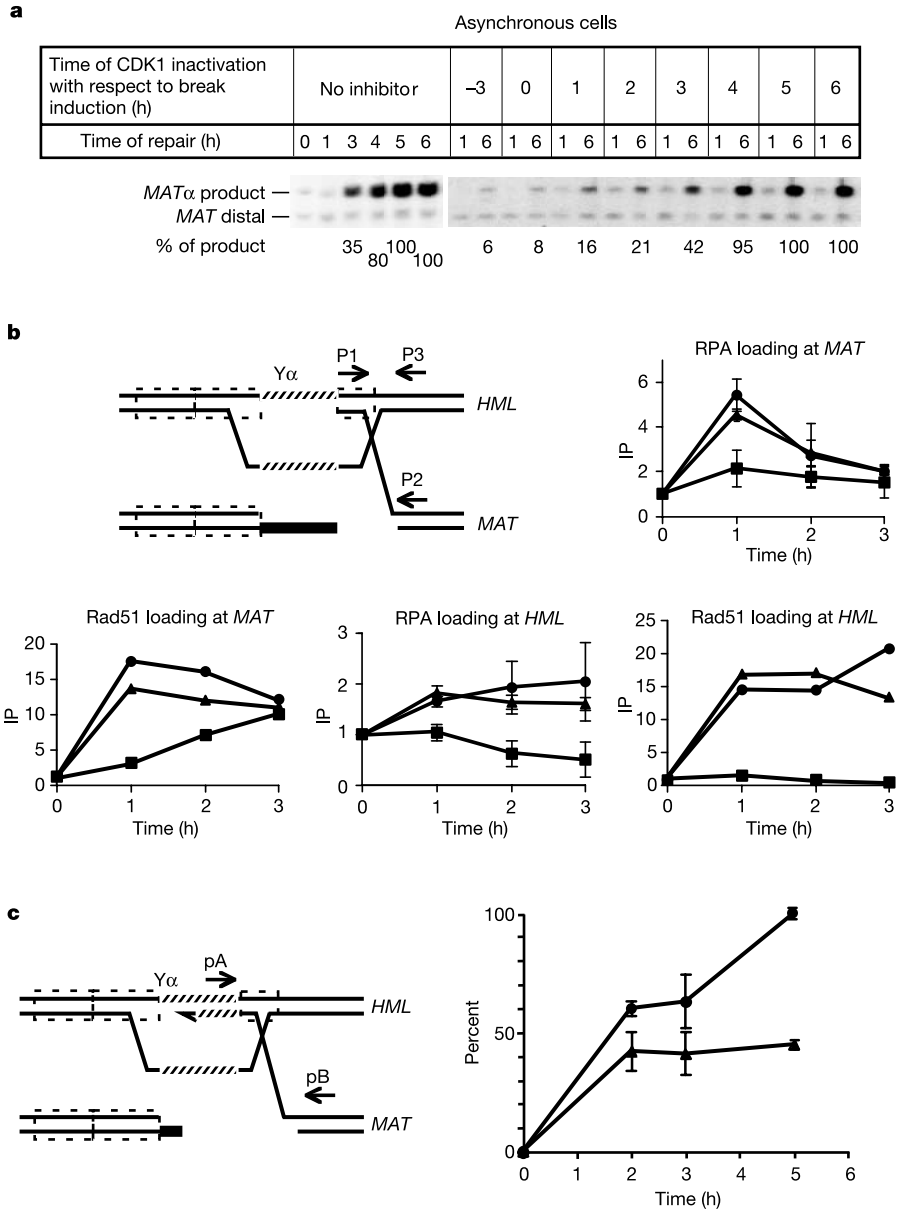

Figure 5 Role of *CDK1* in a late stage of *MAT* switching. **a**, Cdc28-as1 was inhibited in cells at different times before and after *HO* induction, and the amount of product formed at 6 h was determined. **b**, Strand invasion was tested by ChIP analysis for RPA and Rad51 in a *cdc28-as1* strain. The diagram shows homologous sequences (dashed outlined boxes) and primers used to detect immunoprecipitation (IP) of *MAT* (p1, p2) or *HML* (p1, p3) with anti-Rad51 or Rfa1 antibodies. Symbols indicate the time at which inhibitor was added with respect to break induction: triangles, no inhibitor; squares, 0.5 h; circles, 1.5 h. **c**, Polymerase chain reaction detects the first new DNA synthesis primed by the 3′ invading end after strand invasion. Circles, no inhibitor; triangles, 1-NMPP1 added 1.5 h after *HO* induction. Where error bars are shown, results are means ± s.d.

promote a G1-like repair response. Since Mre11 is required both for NHEJ and HR[28], perhaps in CDK1-limiting G2 cells, Mre11 is 'frozen' in a NHEJ-proficient status, unable to resect DSB ends and therefore to generate checkpoint signals. This is also in accordance with observations *in vitro* showing that MRX complexes protect DNA ends from other exonucleases[29]. □

Methods

Strains

Strains used to study DSB ends resection, DNA damage checkpoint activation and NHEJ were derivatives of JKM139 (*hoΔ MAT***a** *hmlΔ::ADE1 hmrΔ::ADE1 ade1-100 leu2-3,112 lys5 trp1Δ::hisG ura3-52 ade3::GAL::HO*) or JKM179 (same genotype except *MAT*α), carrying *GAL1::SIC1* (integrating pMHT plasmid with a stable version of the *SIC1* gene under the *GAL1* promoter[11], kindly provided by J. Diffley); *CHK1-13MYC; DDC-4HA; RAD9-13MYC; mre11Δ; mec1Δsml1Δ; rad50Δ; bar1Δ; cdc28-as1; cdc5-ad* or the combination of these mutations. In *MAT***a**-inc strains the HO recognition site has a 1-bp substitution that prevents HO endonuclease cleavage. The diploid strain used to study DSB-induced checkpoint activation and resection was *MAT***a**/*MAT***a**-like, where part of the Yα sequence was replaced with *KANMX*. *MAT* switching was tested in *MAT***a** *HML*α *HMR***a** *ade3::GAL::HO ade1-100 leu2-3,112 lys5 ura3-52 bar1Δ* strains, some carrying *cdc28-as1* or *cdc7-as3*. In the experiment shown in Fig. 2b, gene conversion from both *HML* and *HMR* yields cells that remain α-factor sensitive because both *HMR* and *HML* contain **Y**a information. In the strain used to study allelic recombination, the recipient chromosome has an insertion of *URA3* at *PHO87* located 5 kb to the left of *MAT*, whereas the donor chromosome has the Yα and Z1 sequences of *MAT*α replaced by *KANMX* and is not cut by HO endonuclease.

Fluorescence-activated cell sorting analysis

Fluorescence-activated cell sorting was performed as described[3].

CDK1 inactivation, α-factor arrest and nocodazole arrest

CDK1 and Cdc7 were inactivated in *cdc28-as1* and *cdc7-as3* strains by adding the ATP analogue inhibitor 1-NMPP1 at 5 μM unless otherwise indicated. In *cdc28-as1*, *cdc7-as3* and wild-type cells, inhibitor was added 1.25 doubling times before inducing *HO* unless otherwise indicated. Cells were arrested in G1 with 10 μg ml^{-1} α-factor (or 0.5 μg ml^{-1} in *bar1Δ* strains). Cells were arrested in G2/M with 20 μg ml^{-1} nocodazole.

HO induction

Strains were grown in YP-lactate (1% Bacto yeast extract, 2% Bacto peptone, 3% lactic acid, pH 5.5) and HO induction was done as described previously[4].

5′-3′ strand resection at a DSB

Resection was measured as a rate of HO-cut band disappearance. In some cases the resection of sequences distant from the break was also measured. Purified genomic DNA, digested with *Eco*RI (Fig. 3) or *Sty*I (Fig. 4), was separated on a 1% agarose gel, transferred to Hybond N^+ and probed with ^{32}P-labelled DNA from *MAT***a** and from sequences 20 kb proximal to the DSB to establish the rate of resection. Hybridization to *HIS4* or *LEU2* (both more than 100 kb away) was used to normalize the amount of DNA at each time point. The rate of resection at each time point was plotted as the percentage of the density of the initial cut band. The density of the HO-cut band at $t = 1$ h was set to 100%.

NHEJ efficiency

NHEJ was examined in a donorless *cdc28-as1* strain. 1-NMPP1 inhibitor was added 30 min before *HO* induction. Re-cutting of *MAT***a** by HO was prevented by filtering cells out of galactose-containing medium 30 min after DSB induction and diluting cells into YP-dextrose. (1% Bacto yeast extract, 2% Bacto peptone, 2% dextrose, pH 5.5). The efficiency of NHEJ was determined as the intensity of the *MAT***a**-containing restriction fragment 3 h after *HO* induction, normalized to the amount of DNA.

Analysis of homologous recombination

MAT switching and other homologous recombination events were analysed on Southern blots[4]. For *MAT* switching, genomic DNA was digested with *Sty*I and *Bgl*II (Fig. 2a) or with *Sty*I (Fig. 2b–d) and probed with a *MAT*-distal probe. For allelic recombination, DNA was digested with *Bgl*II and *Pvu*I and probed with the *MAT*-distal probe to check the efficiency of HO induction and with a *MAT*-proximal probe to check the appearance of the product. Initial new DNA synthesis after strand invasion was determined by polymerase chain reaction as described[4], normalized to the amount of *ARG5,6* DNA.

Chromatin immunoprecipitation

Chromatin immunoprecipitation was performed as described previously[4,6]. Antibodies against Mre11, Rad51 and RPA were provided by J. H. J. Petrini, A. Shinohara and S. Brill, respectively.

Western blots

Protein extracts were performed as described[3]. Antibodies used for western blots were Rad53 polyclonal antibody JD47 (a gift from J. Diffley), Mre11 polyclonal antibody (produced by the IFOM antibody facility) and monoclonal antibodies 9E10 (anti-Myc epitope), 12CA5 (anti-HA (haemagglutinin) epitope) and 6D2 (ref. 11) (anti-B subunit).

Received 1 June; accepted 19 August 2004; doi:10.1038/nature02964.

1. Lee, S. E. *et al. Saccharomyces* Ku70, Mre11/Rad50 and RPA proteins regulate adaptation to G2/M arrest DNA damage. *Cell* **94,** 399–409 (1998).
2. Toczyski, D. P., Galgoczy, D. J. & Hartwell, L. H. CDC5 and CKII control adaptation to the yeast DNA damage checkpoint. *Cell* **90,** 1097–1106 (1997).
3. Pellicioli, A., Lee, S. E., Lucca, C., Foiani, M. & Haber, J. E. Regulation of *Saccharomyces* Rad53 checkpoint kinase during adaptation from G2/M arrest. *Mol. Cell* **7,** 293–300 (2001).
4. Sugawara, N., Wang, X. & Haber, J. E. *In vivo* roles of Rad52, Rad54, and Rad55 proteins in Rad51-mediated recombination. *Mol. Cell* **12,** 209–219 (2003).
5. Vaze, M. B. *et al.* Recovery from checkpoint-mediated arrest after repair of a double-strand break requires Srs2 helicase. *Mol. Cell* **10,** 373–385 (2002).
6. Wang, X. & Haber, J. E. Role of *Saccharomyces* single-stranded DNA-binding protein RPA in the strand invasion step of double-strand break repair. *PLoS Biol.* **2,** 104–111 (2004).
7. Bishop, A. C. *et al.* A chemical switch for inhibitor-sensitive alleles of any protein kinase. *Nature* **407,** 395–401 (2000).
8. Ubersax, J. A. *et al.* Targets of the cyclin-dependent kinase Cdk1. *Nature* **425,** 859–864 (2003).
9. Zou, L. & Elledge, S. J. Sensing DNA damage through ATRIP recognition of RPA-ssDNA complexes. *Science* **300,** 1542–1548 (2003).
10. Nasmyth, K. At the heart of the budding yeast cell cycle. *Trends Genet.* **12,** 405–412 (1996).
11. Pellicioli, A. *et al.* Activation of Rad53 kinase in response to DNA damage and its effect in modulating phosphorylation of the lagging strand DNA polymerase. *EMBO J.* **18,** 6561–6572 (1999).
12. Naiki, T., Wakayama, T., Nakada, D., Matsumoto, K. & Sugimoto, K. Association of Rad9 with double-strand breaks through a Mec1-dependent mechanism. *Mol. Cell. Biol.* **24,** 3277–3285 (2004).
13. Diede, S. J. & Gottschling, D. E. Exonuclease activity is required for sequence addition and Cdc13p loading at a *de novo* telomere. *Curr. Biol.* **11,** 1336–1340 (2001).
14. Caspari, T., Murray, J. M. & Carr, A. M. Cdc2-cyclin B kinase activity links Crb2 and Rqh1-topoisomerase III. *Genes Dev.* **16,** 1195–1208 (2002).
15. Grenon, M., Gilbert, C. & Lowndes, N. F. Checkpoint activation in response to double-strand breaks requires the Mre11/Rad50/Xrs2 complex. *Nature Cell Biol.* **3,** 844–847 (2001).
16. D'Amours, D. & Jackson, S. P. The yeast Xrs2 complex functions in S phase checkpoint regulation. *Genes Dev.* **15,** 2238–2249 (2001).
17. Moore, J. K. & Haber, J. E. Cell cycle and genetic requirements of two pathways of nonhomologous end-joining repair of double-strand breaks in *Saccharomyces cerevisiae*. *Mol. Cell. Biol.* **16,** 2164–2173 (1996).
18. Frank-Vaillant, M. & Marcand, S. Transient stability of DNA ends allows nonhomologous end joining to precede homologous recombination. *Mol. Cell* **10,** 1189–1199 (2002).
19. Karathanasis, E. & Wilson, T. E. Enhancement of *Saccharomyces cerevisiae* end-joining efficiency by cell growth stage but not by impairment of recombination. *Genetics* **161,** 1015–1027 (2002).
20. Liberi, G. *et al.* Srs2 DNA helicase is involved in checkpoint response and its regulation requires a functional Mec1-dependent pathway and Cdk1 activity. *EMBO J.* **19,** 5027–5038 (2000).
21. Sogo, J. M., Lopes, M. & Foiani, M. Fork reversal and ssDNA accumulation at stalled replication forks owing to checkpoint defects. *Science* **297,** 599–602 (2002).
22. Foiani, M., Liberi, G., Lucchini, G. & Plevani, P. Cell cycle-dependent phosphorylation and dephosphorylation of the yeast DNA polymerase α-primase B subunit. *Mol. Cell. Biol.* **15,** 883–891 (1995).
23. Lisby, M., Mortensen, U. H. & Rothstein, R. Colocalization of multiple DNA double-strand breaks at a single Rad52 repair centre. *Nature Cell Biol.* **5,** 572–577 (2003).
24. Rothkamm, K., Kruger, I., Thompson, L. H. & Lobrich, M. Pathways of DNA double-strand break repair during the mammalian cell cycle. *Mol. Cell. Biol.* **23,** 5706–5715 (2003).
25. Lee, J. & Desiderio, S. Cyclin A/CDK2 regulates V(D)J recombination by coordinating RAG-2 accumulation and DNA repair. *Immunity* **11,** 771–781 (1999).
26. Toh, G. W. & Lowndes, N. F. Role of the *Saccharomyces cerevisiae* Rad9 protein in sensing and responding to DNA damage. *Biochem. Soc. Trans.* **31,** 242–246 (2003).
27. Masumoto, H., Muramatsu, S., Kamimura, Y. & Araki, H. S-Cdk-dependent phosphorylation of Sld2 essential for chromosomal DNA replication in budding yeast. *Nature* **415,** 651–655 (2002).
28. D'Amours, D. & Jackson, S. P. The Mre11 complex: at the crossroads of DNA repair and checkpoint signalling. *Nature Rev. Mol. Cell Biol.* **3,** 317–327 (2002).
29. Chen, L., Trujillo, K., Ramos, W., Sung, P. & Tomkinson, A. E. Promotion of Dnl4-catalyzed DNA end-joining by the Rad50/Mre11/Xrs2 and Hdf1/Hdf2 complexes. *Mol. Cell* **8,** 1105–1115 (2001).

Supplementary Information accompanies the paper on **www.nature.com/nature**.

Acknowledgements The order of the co-first authors (G.I. and A.P.) and the order of the second two authors (A.B. and X.W.) were decided alphabetically. A.B. and X.W. made substantial and equal contributions to this work. We thank C. Zhang and K. Shokat (supported by NIH grant AI44009) for the *cdc28-as1* allele and the 1-NMPP1 inhibitor. We note the ownership of the ASKA technology by Cellular Genomics Inc. and thank CGI for granting us the rights to perform the experiments discussed in the publication. We thank J. Petrini, J. Diffley, K. Labib, M. P. Longhese, S. Brill and the IFOM antibody facility for reagents. We are grateful to C. Lucca, E. Pandiani, M. B. Vaze, S. Francia, S. Lovett, M. Lichten and the members of our laboratories for discussions and technical support. N.M.H. was supported by the NIH. M.F. and A.P. were supported by grants from Associazione Italiana per la Ricerca sul Cancro and M.F. from Telethon-Italy and the European Community. G.I. was supported by Charles A. King Trust Postdoctoral Fellowship. G.I. is on leave from N. Copernicus University, Torun, Poland. J.E.H. was supported by the NIH and the DOE.

Competing interests statement The authors declare that they have no competing financial interests.

Correspondence and requests for materials should be addressed to M.F. (marco.foiani@ifom-ieo-campus.it) or J.E.H. (haber@brandeis.edu).

erratum

High-resolution structure of a retroviral capsid hexameric amino-terminal domain

Gulnahar B. Mortuza, Lesley F. Haire, Anthony Stevens, Stephen J. Smerdon, Jonathan P. Stoye & Ian A. Taylor

Nature **431,** 481–485 (2004).

In this Letter, the following sentence should have appeared after the author's email address: 'Coordinates and structure factors have been deposited in the Protein Data Bank under accession number 1U7K.'. □